

## pd scattering at 250 MeV and three-nucleon forces

K. Hatanaka<sup>1,a</sup>, J. Kamiya<sup>1</sup>, Y. Maeda<sup>2</sup>, T. Noro<sup>3</sup>, K. Sagara<sup>3</sup>, H. Sakai<sup>2</sup>, Y. Sakemi<sup>1</sup>, K. Sekiguchi<sup>2</sup>, Y. Shimizu<sup>1</sup>, A. Tamii<sup>2</sup>, T. Wakasa<sup>1</sup>, K. Yako<sup>2</sup>, H.P. Yoshida<sup>1</sup>, and V.P. Ladygin<sup>4</sup>

<sup>1</sup> Research Center for Nuclear Physics, Osaka University, Ibaraki, Osaka 567-0047, Japan

<sup>2</sup> Department of Physics, University of Tokyo, Bunkyo, Tokyo 113-0033, Japan

<sup>3</sup> Department of Physics, Kyushu University, Hakozaki, Fukuoka 812-8581, Japan

<sup>4</sup> Joint Institute for Nuclear Researches, 141980 Dubna, Russia

Received: 30 September 2002 /

Published online: 22 October 2003 – © Società Italiana di Fisica / Springer-Verlag 2003

**Abstract.** We have measured angular distributions of the differential cross-section, the analyzing power and all of the spin transfer coefficients  $K_y^{y'}$ ,  $K_x^{x'}$ ,  $K_z^{z'}$ ,  $K_x^{z'}$ , and  $K_z^{x'}$  for the pd elastic scattering at 250 MeV. These are the first measurements of a complete set of proton polarization observables for pd elastic scattering at intermediate energies. The present data are compared with theoretical predictions based on exact solutions of the three-nucleon Faddeev equations and modern realistic nucleon-nucleon potentials combined with three-nucleon forces (3NF), namely the Tucson-Melbourne (TM)  $2\pi$ -exchange model, a modification thereof (TM') closer to chiral symmetry, and the Urbana IX model.

**PACS.** 21.45.+v Few-body systems – 21.30.-x Nuclear forces – 24.70.+s Polarization phenomena in reactions

### 1 Introduction

Studies of few-nucleon systems offer a good opportunity to investigate the nature of nuclear forces. Owing to intensive theoretical and experimental efforts, a so-called new generation of realistic nucleon-nucleon (NN) potentials has been obtained using meson-exchange or other more phenomenological approaches, namely AV18 [1], CD Bonn [2], Nijm I, II and 93 [3]. They describe the rich set of experimental NN data up to 350 MeV which is well above the pion threshold of 290 MeV. These realistic two-nucleon forces (2NF), however, fail to reproduce experimental binding energies for light nuclei where rigorous solutions of the Schrödinger equation are available, clearly showing underbinding. For instance, the underbinding amounts to 0.5–1 MeV in the case of  $^3\text{H}$  and  $^3\text{He}$  and to 2–4 MeV in the case of  $^4\text{He}$ . One can achieve correct three-nucleon (3N) and four-nucleon (4N) binding energies by including the Tucson-Melbourne (TM) [4] or Urbana IX [5] three-nucleon forces (3NF) which are refined versions of the Fujita-Miyazawa force [6], a  $2\pi$ -exchange between three nucleons with an intermediate  $\Delta$  excitation. In recent years, it became possible to perform rigorous numerical Faddeev-type calculations for the 3N scattering processes by the advances in computational capabilities.

In addition to the first signal on 3NF effects resulting from discrete states, strong 3NF effects were observed

in a study of the minima of the Nd elastic scattering cross-section at incoming nucleon energies higher than about 60 MeV [7]. On the other hand, a recent study at RIKEN [8] shows that the inclusion of the 3NF does not always improve the description of precise data taken at intermediate deuteron energies. Proton vector analyzing power data at 70–200 MeV have revealed the deficiency of 3NF [9,10], which produces large but wrong effects. These results may be caused by a wrong spin structure of present-day 3NF. Clearly, the present situation is only the very beginning of the investigation of the spin structure of the 3NF. In addition, one can expect relativistic effects with increasing energy. However, the existing higher-energy database for the proton analyzing power is rather poor. There are no measurements of two-spin observables except for the spin correlation coefficient  $C_{yy}$  at 197 MeV at IUCF [11]. Precise data at intermediate energies including higher-rank spin observables are needed to provide constraints on theoretical 3NF models.

In the present study, we have measured angular distributions of the differential cross-section, the analyzing power  $A_y$  and all proton spin transfer coefficients  $K_x^{x'}$ ,  $K_z^{z'}$ ,  $K_x^{z'}$ ,  $K_z^{x'}$ , and  $K_y^{y'}$  for pd elastic scattering at 250 MeV. This energy is slightly above the pion threshold at 215 MeV. Realistic NN potentials have been obtained by analyzing the existing NN database up to 350 MeV. The corresponding proton energy in the pd system is 259 MeV to give the same center-of-mass (c.m.) energy.

<sup>a</sup> e-mail: [hatanaka@rcnp.osaka-u.ac.jp](mailto:hatanaka@rcnp.osaka-u.ac.jp)

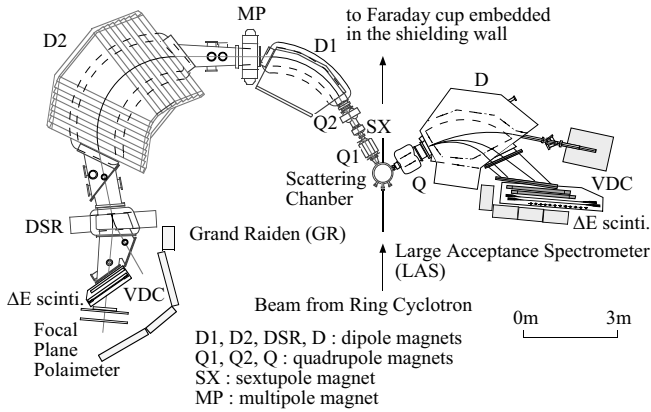


**Fig. 1.** Schematic layout of the RCNP dual spectrometer consisting of Grand Raiden and LAS.

Most of the effects caused by the pion production are expected to be taken into account in the realistic NN potentials. The cross-section of elastic pd scattering shows a smooth energy dependence in the 200–300 MeV range indicating a small effect of the pion production and a possibly larger relativistic effect in this energy region [12].

## 2 Experimental results and discussions

The experiment was performed at the Research Center for Nuclear Physics (RCNP), Osaka University. Polarized protons were produced in an atomic beam polarized ion source [13], injected into and accelerated by the  $K = 120$  MeV AVF (azimuthally varying field) cyclotron up to 46.7 MeV. Subsequently the beam was injected into the  $K = 400$  MeV ring cyclotron and accelerated to the final energy of 250 MeV. The polarization axis was vertical after the AVF cyclotron. Two superconducting solenoids located in the beam transfer line between the AVF cyclotron and the ring cyclotron were used to precess the proton spin polarization into the horizontal plane so as to have either of the two spin states sideways or longitudinal on the target. The proton polarization was continuously measured with two beamline polarimeters separated by a total bending angle of  $115^\circ$ , precessing the spin of 250 MeV protons by about  $260^\circ$  between the two polarimeters. Both the horizontal and vertical components of the polarization vector were determined. During the measurements, typical values for polarization and beam current were 70% and 200 nA, respectively. Analyzing power of the beamline polarimeter was precisely determined to be  $0.362 \pm 0.003$  at the laboratory angle of  $17^\circ$  [14].

Measurements were performed using self-supporting 99% isotopically enriched deuterated polyethylene foils ( $\text{CD}_2$ ) with total thicknesses of 21 and 44  $\text{mg}/\text{cm}^2$ . A 15  $\text{mg}/\text{cm}^2$  thick, natural carbon target was used to subtract contributions due to scattering on carbon. It is essential to get precise absolute cross-sections for comparison with Faddeev calculations. Therefore, in a later measurement, a gaseous  $\text{D}_2$  target was used to normalize cross-sections taken with the solid  $\text{CD}_2$  target. The uncertainty

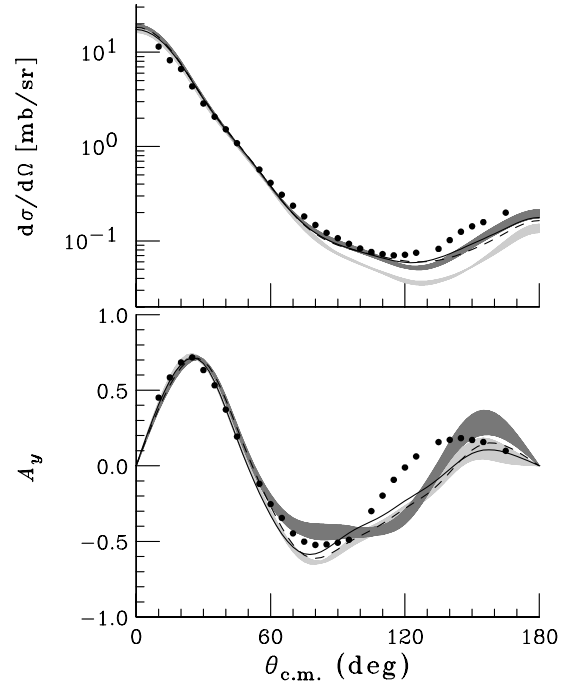


**Fig. 2.** The differential cross-section  $d\sigma/d\Omega$  (top) and proton analyzing powers (bottom) of elastic pd scattering at  $E_p = 250$  MeV. The light-shaded bands contain NN force predictions (AV18, CD-Bonn, Nijm I, II, and 93); the dark-shaded bands contain the NN + TM 3NF predictions. The solid and dashed lines are the AV18 + Urbana IX and CD-Bonn + TM' predictions, respectively.

in the overall normalization was estimated to be 3% by comparing pp scattering data with calculations by the phase-shift analysis program code SAID.

Scattered protons or recoil deuterons in the pd scattering were momentum analyzed by the Grand Raiden spectrometer [15]. The layout of the system is shown in fig. 1. The LAS spectrometer was used to monitor the luminosity. The polarization transfer (PT) coefficients ( $K_i^{j'}$ ) are defined by the following relation:

$$\begin{pmatrix} p'_{x'} \\ p'_{y'} \\ p'_{z'} \end{pmatrix} = \frac{1}{1 + p_y A_y} \times \left[ \begin{pmatrix} 0 \\ P_{y'} \\ 0 \end{pmatrix} + \begin{pmatrix} K_x^{x'} & 0 & K_z^{x'} \\ 0 & K_y^{y'} & 0 \\ K_x^{z'} & 0 & K_z^{z'} \end{pmatrix} \begin{pmatrix} p_x \\ p_y \\ p_z \end{pmatrix} \right], \quad (1)$$

where  $p_i$  and  $p'_{j'}$  ( $i$  or  $j = x, y, z$ ) denote the polarization of the incident and scattered protons, respectively. The polarization of elastically scattered protons from  $\text{CD}_2$  targets was measured by the FPP after momentum analysis in the Grand Raiden spectrometer (fig. 1). Detailed descriptions are found in ref. [16] about the procedures to measure the PT coefficients.

The experimental results for the differential cross-section ( $d\sigma/d\Omega$ ), the vector analyzing power ( $A_y$ ) and the PT coefficients ( $K_x^{x'}$ ,  $K_x^{z'}$ ,  $K_z^{x'}$ ,  $K_z^{z'}$ , and  $K_y^{y'}$ ) are shown in figs. 2 and 3. The quoted errors are statistical

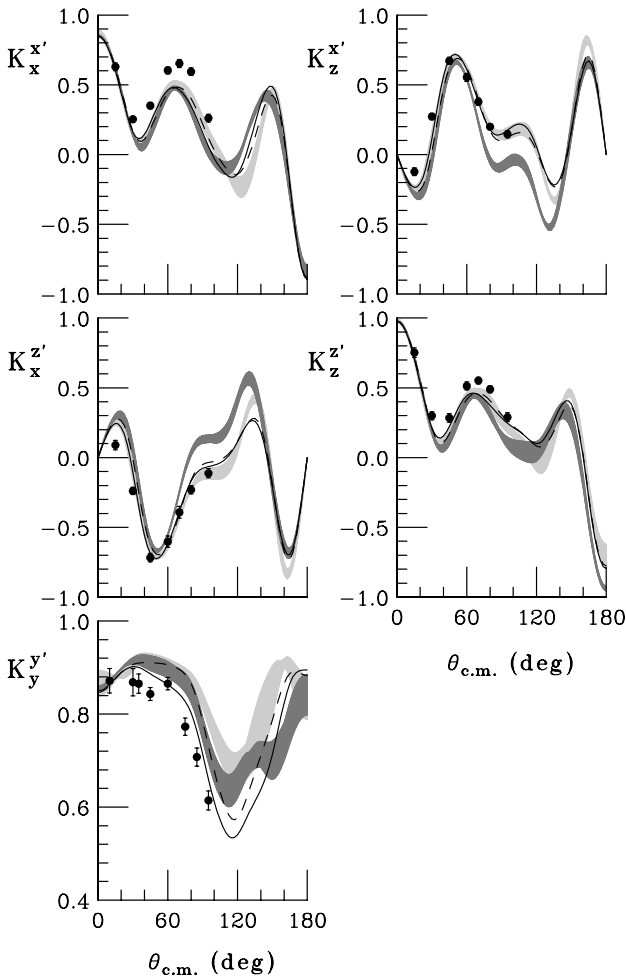


**Fig. 3.** Polarization transfer coefficients ( $K_x^{x'}$ ,  $K_x^{z'}$ ,  $K_z^{x'}$ ,  $K_z^{z'}$ , and  $K_y^{y'}$ ) of elastic pd scattering at  $E_p = 250$  MeV. For the description of bands and lines see legend of fig. 2.

ones only. The overall uncertainty in the absolute normalization of the cross-section is estimated to be 3% from the calibration by the gaseous target measurements as previously described. There is also the relative uncertainty of 2.5% attributed to the inhomogeneity of CD<sub>2</sub> foils. The analyzing power has an uncertainty of 1% in the absolute normalization owing to the precise calibration of the beamline polarimeter in this experiment. The PT coefficients have an uncertainty of 2.5% in the normalization due to the uncertainty of the effective analyzing power of the FPP. For the PT coefficients, axes  $\hat{i}$  and  $\hat{j}'$  are defined in the laboratory scattering frame and  $K_i^{j'}$  are plotted as function of the c.m. angles.

In the top panel of fig. 2, the measured differential cross-section is compared with rigorous Faddeev solutions by H. Kamada [17]. The various 2NF predictions are very similar and are depicted by a narrow band (light shaded), which reflects the small dependence on the particular NN interaction used. The inclusion of the TM 3NF (dark-shaded band) leads to a much better description at angles larger than 70°. This supports the claim of the clear evidence [7,8] of the 3NF from the systematic analysis of the

energy dependence of the cross-section data. The inclusion of the TM' (dashed curve) and the Urbana IX (solid curve) 3NF also leads to a good agreement to the data. However, discrepancies remain at angles larger than 120°. From the analysis of the dp data at the equivalent proton energy of 135 MeV [8], it has been shown that the TM 3NF and the Urbana IX 3NF provided a good description of the cross-section even at very backward angles.

In the bottom panel of fig. 2, we compare the experimental analyzing power  $A_y$  with different nuclear-force predictions. The differences (narrow light-shaded band) between the 2NF predictions are rather small at forward angles and become larger at backward angles. These predictions are in good agreement with the experimental data at forward angles, but deviate dramatically at backward angles larger than 60°. The experimental analyzing power  $A_y$  changes the sign at about 120°, while the calculations predict this change only around 140°. In the angular range 60°–120°, 2NF predictions are clearly larger in absolute value than experimental data. By including the TM 3NF (dark-shaded band) the agreement with the data becomes better in the minimum around  $\theta_{c.m.} = 60^\circ$ – $100^\circ$  but the discrepancies at more backward angles remain. This is again in contrast to the results for the deuteron vector analyzing power as shown in ref. [8], where predictions with the TM 3NF describe the data very well not only in the minimum but also at backward angles.

Our PT data are shown in fig. 3 together with theoretical predictions. The PT coefficients in the horizontal plane ( $K_x^{x'}$ ,  $K_x^{z'}$ ,  $K_z^{x'}$ , and  $K_z^{z'}$ ) are reasonably well described by calculations with 2NF only (light-shaded bands). The inclusion of the TM 3NF (dark-shaded bands) rather deteriorates the agreement with the experimental data. The TM' (dashed curves) and the Urbana IX (solid curves) 3NF do not have a large effect on these PT coefficients and give a reasonably good agreement with the data. In the case of the PT coefficient in the vertical plane ( $K_y^{y'}$ ), the inclusion of the TM 3NF (dark-shaded band) and especially the Urbana IX 3NF (solid curve) give results in better agreement with the measurements. This is similar to the case of the analyzing power which is also a polarization observable in the vertical plane. Present measurements were limited to relatively forward angles  $\theta_{c.m.} \leq 95^\circ$ . In fig. 3, large differences are observed between theoretical predictions with and without 3NFs at more backward angles for some PT coefficients. At angles larger than 100°, the energies of scattered protons are less than 120 MeV, where the present FPP at the Grand Raiden has a poor efficiency [16]. A low-energy FPP is now under development at the RCNP to enable measurements of proton polarization below 120 MeV.

At intermediate energies, our data are the first complete set of PT coefficients for pd elastic scattering covering a wide angular range and serve as a good testing ground of the investigation of the spin structure of 3NF and the effects of relativity. In order to offer further valuable sources of information, a rich spectrum of spin observables will be measured not only for elastic scattering

but also for the Nd breakup process. For both of them, large 3NF effects have been predicted at higher energies.

## References

1. R.B. Wiringa *et al.*, Phys. Rev. C **51**, 38 (1995).
2. R. Machleidt *et al.*, Phys. Rev. C **53**, R1483 (1996).
3. V.G.J. Stoks *et al.*, Phys. Rev. C **49**, 2950 (1994).
4. S.A. Coon, M.T. Peña, Phys. Rev. C **48**, 2559 (1993).
5. B.S. Pudliner *et al.*, Phys. Rev. C **56**, 1720 (1997).
6. J. Fujita, H. Miyazawa, Prog. Theor. Phys. **17**, 360 (1957).
7. H. Witała *et al.*, Phys. Rev. Lett. **81**, 1183 (1998).
8. K. Sekiguchi *et al.*, Phys. Rev. C **65**, 034003 (2002).
9. E.J. Stephenson *et al.*, Phys. Rev. C **60**, 061001(R) (1999).
10. K. Ermisch *et al.*, Phys. Rev. Lett. **86**, 5862 (2001).
11. R.V. Cadman *et al.*, Phys. Rev. Lett. **86**, 967 (2001).
12. H. Rohdjeß *et al.*, Phys. Rev. C **57**, 2111 (1998).
13. K. Hatanaka *et al.*, Nucl. Instrum. Methods Phys. Res. A **384**, 575 (1997).
14. K. Hatanaka *et al.*, to be published in *IX Workshop on High Energy Spin Physics, Spin-01, Dubna, August 2-7, 2001* (The Bogoliubov Laboratory of Theoretical Physics, JINR).
15. M. Fujiwara *et al.*, Nucl. Instrum. Methods Phys. Res. A **422**, 484 (1999).
16. T. Kawabata *et al.*, Phys. Rev. C **65**, 064316 (2002).
17. H. Kamada, private communication.